

血行再建術を用いた脳動脈瘤治療における Balloon test occlusion の有用性と問題点

清水 宏明¹, 松本 康史², 江面 正幸³
高橋 明³, 富永 悌二⁴

Balloon Test Occlusion as a Preoperative Evaluation for Cerebral Aneurysms Treated with Bypass Surgery

Hiroaki SHIMIZU, M.D.,¹ Yasushi MATSUMOTO, M.D.,² Masayuki EZURA, M.D.,³
Akira TAKAHASHI, M.D.,³ and Teiji TOMINAGA, M.D.⁴

Departments of ¹Neurosurgery and ²Neuroendovascular Therapy, Kohnan Hospital, and
Department of ³Neuroendovascular Therapy and ⁴Neuroendovascular, Tohoku University
Graduate School of Medicine, Sendai, Japan

Summary: For the treatment of patients with complex internal carotid artery (ICA) aneurysms, it may be necessary to occlude the parent artery following a bypass surgery. The bypass surgery may be low or high flow bypass, but selection criteria have not been established. We retrospectively analyzed our method using preoperative balloon test occlusion (BTO).

Thirty-five patients with ICA aneurysms, 15 ruptured and 20 unruptured, were treated with parent artery occlusion with bypass surgery. Preoperative BTO was performed in 27 cases (all unruptured and 7 ruptured, chronic stage cases). When ischemic symptoms occurred during BTO, high flow bypass was performed followed by parent artery occlusion. Otherwise, single-photon emission computed tomographic findings during BTO were used for the bypass selection. If ipsilateral residual blood flow was 70–75% or less of the contralateral hemisphere, high flow bypass was chosen and if between 70–75% and 90%, superficial temporal artery-middle cerebral artery (STA-MCA) bypass was employed. In the acute stage of 8 ruptured cases, BTO was not performed and bypass selection was made according to angiographic findings only. After completion of the bypass, ipsilateral ICA occlusion (ICO) was performed either by direct or intravascular technique. The site of ICO was determined to completely block the blood flow into the aneurysm considering both conventional angiography and BTO findings.

A total of 15 STA-MCA and 20 high flow bypasses were performed followed by ICO. There was no mortality or morbidity in unruptured cases. In ruptured cases, there were 3 complications related to surgical procedure such as perforator injury, but no patients showed insufficient ipsilateral cerebral blood flow postoperatively. One asymptomatic cerebral infarction developed due to BTO. In 5 cases, petrous portion collateral flow from external to internal carotid artery was seen, and the ICO was performed above the collateral using intravascular embolization.

Key words:

- ・ balloon test occlusion
- ・ bypass
- ・ complex aneurysm
- ・ internal carotid artery

Surg Cereb Stroke

(Jpn) 34: 317–322, 2006

¹ 広南病院 脳神経外科, ² 同 血管内脳神経外科, ³ 東北大学大学院 神経病態制御学分野, ⁴ 同 神経外科学分野 (受稿日 2006. 1. 16) (脱稿日 2006. 2. 10) (連絡先: 〒982-8523 宮城県仙台市太白区長町南4-20-1 広南病院 脳神経外科 清水宏明) [Address correspondence: Hiroaki SHIMIZU, M.D., Department of Neurosurgery, Kohnan Hospital, 4-20-1 Nagamachi-minami, Taihaku-ku, Sendai, Miyagi 982-8523, Japan]

In patients with complex ICA aneurysms to be treated with bypass surgery and ICO, BTO may provide a reliable tool to determine the bypass method and the site of ICO.

はじめに

クリッピングも瘤内塞栓も困難な内頸動脈(IC)瘤に対し、治療的内頸動脈閉塞術(ICO)が必要な場合がある³⁾⁴⁾¹⁰⁾¹³⁾。単にICOを行うと1/3前後に虚血性脳障害が生ずるとされ、balloon test occlusion (BTO)で症状が出なかった症例においても3.3-10%に脳梗塞が生じたと報告されている⁶⁾。したがって、ICOにあたって、正常脳を灌流する親動脈にかわる血行をあらかじめバイパス術により確保することが多い(bypass+ICO)。バイパス術式として、浅側頭動脈(STA)-中大脳動脈(MCA)バイパス術やsaphenous vein graftあるいはradial artery graftを用いたhigh flowバイパス術があるが、その選択方法に関する十分な検討はなされていない。

当科では、ICOに伴うバイパス術の必要性和術式選択についてBTOを用いて判断してきた。今回、bypass+ICOを施行した症例をretrospectiveに検討し、BTOの役割と問題点に関し文献的考察を含めて報告する。

対象と方法

対象は、最近5年間に経験したbypass+ICOにより治療した内頸動脈瘤35例であり、女性32例、男性3例、年齢は35-73歳、平均58歳である。20例は未破裂動脈瘤、15例は破裂動脈瘤であった。動脈瘤の部位は、未破裂では海面静脈洞部14、眼動脈分岐部4、上下垂体動脈分岐部2、破裂では海面静脈洞部2(鼻血1、動静脈瘻1)、眼動脈分岐部3、上下垂体動脈分岐部3、C2部5、後交通動脈分岐部2であった。未破裂例の症状は眼球運動障害15、視力低下5、三叉神経痛3、画像上の増大1であった(重複あり)。

バイパス術の必要性や術式選択のため、未破裂例や破裂後慢性期例では術前にBTOを施行した(27例)。ヘパリン5000IUの静脈内投与下に、7Frの親カテを通じて5FrのモイヤンバルーンカテーテルをIC内に導入し、ICのテスト閉塞を行った。明らかな虚血症状が出現すれば、その時点でテスト終了とし、再開通した。明らかな症状が出なければ、約10分間閉塞を継続し、この間に局所脳酸素飽和度(rSO_2)、短潜時体性感覚誘発電位(SEP)の測定と症状観察を繰り返しつつ、遮断中の側副血行をみるために3ないし4 vessel angiographyを行った。その後スペクト室に移動し、acetazolamide 1gを静注し、8分後にICを再度テスト閉塞し、^{99m}Tc-L,L-ethyl cysteinyl dimer (ECD)

を静注した。静注後IC遮断を解除し、スペクト画像収集を行った。

バイパス術選択は原則として、BTOに伴い虚血症状が出る場合はhigh flowバイパス術とし、虚血症状が出ない場合は、BTO中に行ったECDスペクトにて決定した。すなわち数個の関心領域のいずれかにおいて対側の約70-75%未満に血流が低下する場合はhigh flowバイパス術、70-75%以上90%未満の場合はSTA-MCAバイパス術を原則とした。すべての領域で90%以上の場合はバイパスなしも可としたが年齢などを考慮して決定することとした(対象期間中に2例あったが今回の症例には含めなかった)。

破裂例の急性期手術(8例)では、頸動脈を頸部で用手圧迫して施行した血管撮影上の側副血行を定性的に評価しバイパス術を選択した。BTOを行った症例との比較のため検討に加えた。

バイパス術は、原則としてM2のうち側頭葉を灌流する枝が分岐した直後のM3をrecipientとした。術中血管撮影を用い、吻合完成後にただちにICOを行い、その後止血を確認して閉鎖した。ICOの部位は、原則として海面静脈洞部では頸部内頸動脈結紮、それ以外の部位では瘤近傍で血管内塞栓やクリップを用いてICごと閉塞した。BTO中の同側総頸動脈撮影でのみ確認できるEC-IC間の頭蓋底付近の側副血行路がみられる場合¹⁾¹²⁾、この側副血行がICに合流する部位より末梢で血管内塞栓によりICOを行った。

結 果

15例にSTA-MCAバイパス術、20例にhigh flowバイパス術を施行した。退院時Glasgow outcome scale (GOS)はgood recovery (GR) 29, moderate disability (MD) 3, severe disability (SD) 3であった。そのうち、未破裂の20例では全例でBTOを行い、9例にSTA-MCAバイパス術、11例にhigh flowバイパス術を施行、退院時GOSは全例GRであった。術前症状のうち眼球運動障害と視力低下は改善したが一部残存、三叉神経痛は消失した。破裂15例では慢性期の7例でBTOを施行、急性期8例ではBTOを行わず、6例にSTA-MCAバイパス術、9例にhigh flowバイパス術を施行した。退院時GOSはGR 9, MD 3, SD 3であった。予後不良原因は、くも膜下出血による脳障害(primary injury) 3, 手術合併症3(頭蓋内内頸動脈閉塞に伴う穿通枝障害1, clipping中に動脈瘤から出血

し親動脈閉塞後にバイパスを施行した症例における一時遮断による脳虚血1, 血管内手技に伴う末梢への塞栓1)であった。

BTOに伴う合併症は、症候性のものはなく、無症候性大脳皮質梗塞を1例(4%)に認めた。

5例において、BTO中の同側総頸動脈撮影で外頸-内頸動脈間の頭蓋底付近の側副血行路がみられ¹²⁾、この合流部位より末梢で血管内塞栓によりICOを行った。

代表症例をFig. 1-3に示す。Fig. 1はSTA-MCAバイパス術後ICOを行った典型例を示す。Fig. 2, 3は、いずれもBTOでhigh flowバイパス術が必要と判定された海綿静脈洞部動脈瘤であり、Fig. 2ではバイパス術後、頸部頸動脈結紮のみで治療したが、Fig. 3の症例では外頸-内頸動脈間の頭蓋底付近の側副血行路のため、頸動脈閉塞は血管内手技を用いてこの側副血行路も閉塞できる位置で行った。

考 察

クリッピング、瘤内塞栓のいずれも困難な内頸動脈瘤に対するbypass+ICOの報告は多いが³⁾⁴⁾¹⁰⁾¹³⁾、バイパス術の必要性や術式選択規準、ICOの部位と方法などにつき、まとまった検討はなされていない。

急性ICOに伴う虚血性合併症は26-49%に生ずるとされ¹⁾⁶⁾、従来臨床的BTO(症状出現の有無を指標としたBTO)で症状が発現する場合にあらかじめバイパス術を施行することが勧められた¹¹⁾。しかし、臨床的BTOのfalse negative, すなわち症状が出現しなくてもICO後脳梗塞が出現する頻度は3.3-10%程度に及ぶことが報告され⁶⁾、症状以外の指標が必要とされてきた。症状とDSA上の造影遅延を指標にしたところ、いずれもない場合にはバイパス術なしでも虚血性合併症はないが、症状がなくても造影遅延がある場合はバイパス術を行うべきことを示唆する報告¹⁵⁾や、BTO時患側CBFが30 ml/100 g/min以上あれば、ICOにより脳梗塞を生じないとの報告がある²⁾⁷⁾。ただし、これらは、ICOによる直接の症状や梗塞の有無を問題としており、これらがなくても慢性脳虚血が残存する可能性については議論されていない。われわれは、無症候性であっても高度の血流低下が将来の脳梗塞発生のリスクを上げたり⁹⁾、高次脳機能障害をきたす可能性が否定できない現状では、できるだけ脳血流を維持するためのバイパス術を併用すべきと考えている。

一方、なんらかの指標に基づいてバイパス術を行う場合、術式の選択肢には、STA-MCAバイパス術やsaphenous vein graftあるいはradial artery graftを用いたhigh flowバイパス術があり、一長一短がある。STA-MCAは簡便で安全性も高いが、供給できる血流量はICAの血流量よりかなり少ない範囲にとどまる。high flowバイパス術で

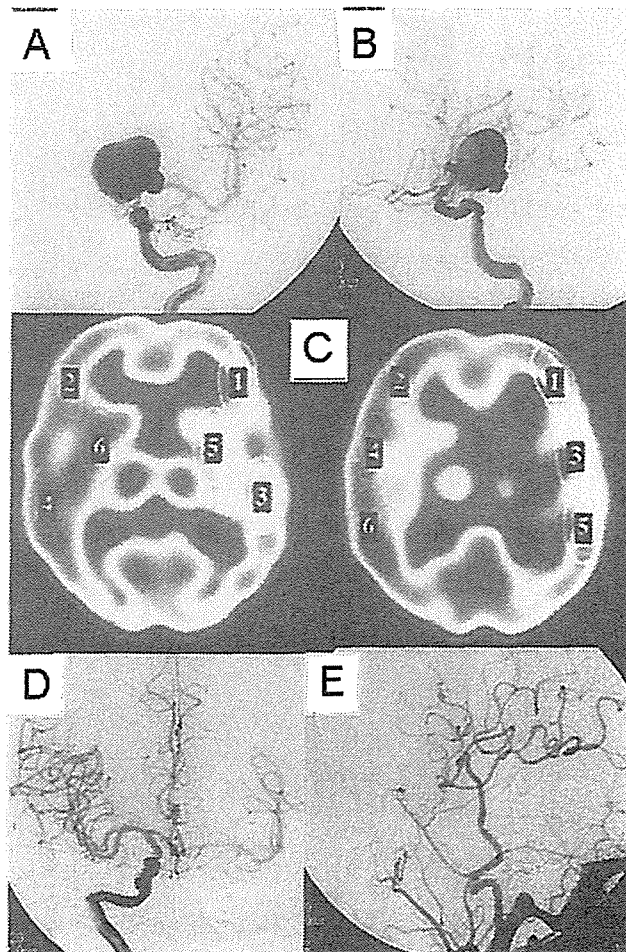


Fig. 1 A 63-year-old man who had left visual disturbance. A and B: Left internal carotid angiography showing a giant paraclinoid internal carotid artery (ICA) aneurysm. C: A ^{99m}Tc-L,lethyl cysteinyl dimer (ECD) SPECT during balloon test occlusion (BTO) of left (right of the figure) ICA showing modest flow reduction in the left cerebral hemisphere (residual flow >75% of the contralateral region in all the regions of interest). D: Right ICA angiography during BTO of left ICA showing moderate collateral flow through anterior communicating artery. E: Postoperative left common carotid arteriography showing patent superficial temporal-middle cerebral artery bypass and no opacification of the aneurysm.

はICAにみあった血流量が供給できるが、手術手技はより煩雑となる。いずれを採用すべきかを決定する手段についてまとまった報告はこれまでみられない。

今回の検討で、われわれはBTO時の症状とSPECT所見に基づいてバイパス術の施行の有無と種類を選択した。選択したバイパス術でバイパス血流不足を生じた例はなく、high flowバイパス術群、STA-MCAバイパス術群のいずれも短期成績は良好であった。したがって今回の選択基準では、少なくとも十分な安全域を持って血行再建を行

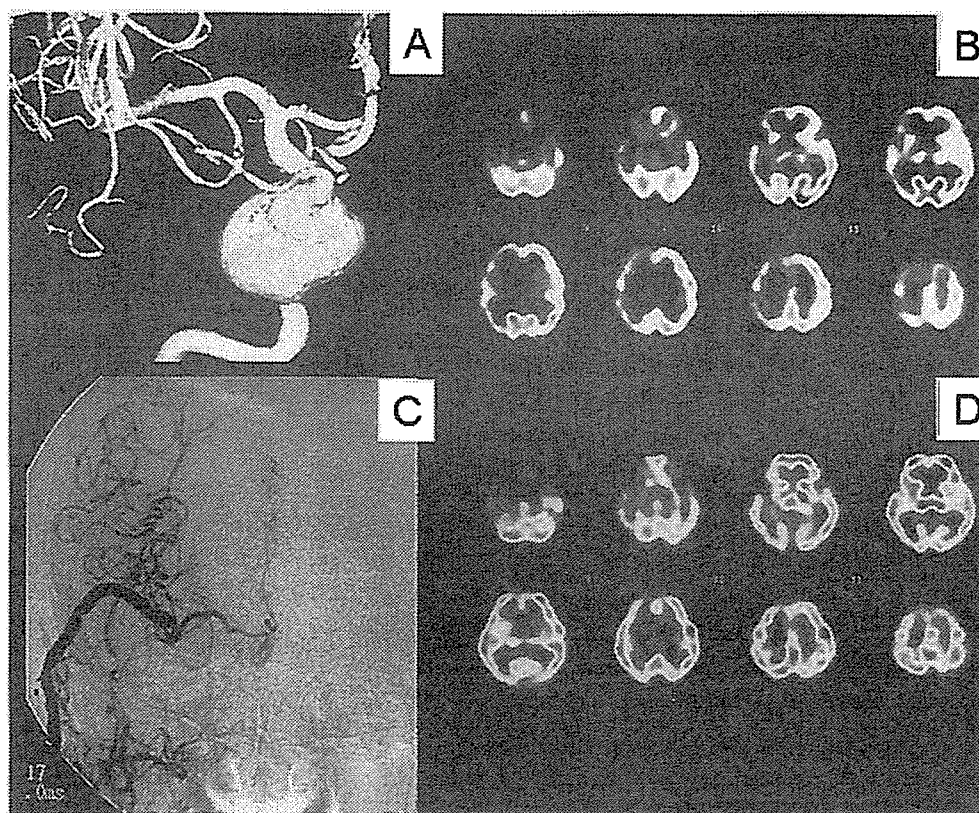


Fig. 2 A 60-year-old woman who complained of diplopia due to right sixth cranial nerve palsy. A: A 3-dimensional digital subtraction angiography (3DDSA) showing a giant right ICA aneurysm at the cavernous portion. B: An ECD SPECT during BTO of right ICA showing marked flow reduction in the right (left of the figure) cerebral hemisphere (residual flow < 70% of the contralateral region). C: An angiography after surgery of external carotid-right middle cerebral artery bypass using saphenous vein graft and ligation of right ICA at the neck. The right intracranial carotid system is opacified through the vein graft and the aneurysm is not seen. D: An ^{123}I -isopropyl-p-iodoamphetamine (IMP) SPECT obtained next day of the surgery showing sufficient flow in the right cerebral hemisphere.

いえたものと思われたが、必要なバイパス血流量を overestimate していた可能性は残る。また、BTO 中の残存血流量が対側の 90% 以上である場合にはバイパスなしで ICO 可能としたが、ICO 後の血行力学的ストレスによる動脈瘤形成の報告もあり¹⁶⁾、バイパス術の risk-benefit を年齢などの点から十分検討する必要があると思われる。すなわち、若年者ではバイパス術を施行するメリットが大きく、高齢者ではバイパス術のリスクのほうが高い場合もあるものと思われるが今後の検討課題である。

BTO のリスクについて、文献的には合併症 3.2-3.7%、うち永続的障害が 0.4-1.7% と報告されており⁵⁾⁸⁾¹⁴⁾、本シリーズでも無症候性梗塞が 1 例に生じた。BTO の必要性や安全性に関する検討は今後も必要であると思われる。また、全体の成績を上げるには、バイパス術に伴う合併症を極力抑制することが必須となることはいうまでもない。vein graft を用いた high flow バイパス術の技術的な要点

としては、適切な graft の採取、recipient の選択、術中血管撮影の使用、静脈のねじれの予防、吻合完成直後の ICO 施行、などが重要と思われた。

ICO の部位と方法に関しては、ICO に伴う EC-IC 間の側副血行を BTO の際に十分評価しておく必要がある。硬膜内動脈瘤の ICO に際しては、眼動脈を介する EC から IC への側副血行を遮断できる部位で ICO を行う必要がある。多くの場合、clip により proximal occlusion ないし trapping するか、瘤内から neck 付近の IC を血管内的に塞栓することになる。この場合、術前の BTO では実際には閉塞される眼動脈の血流を残した状態での評価となることがほとんどであり、解釈に十分な注意が必要である。また、硬膜内動脈瘤では ICO の部位によって穿通枝障害の問題が生ずる。IC の末梢、とくに後交通動脈に近ければ近いほど穿通枝障害が問題になりやすいため、この部位の動脈瘤はできるだけクリッピングを優先し、bypass+ICO は

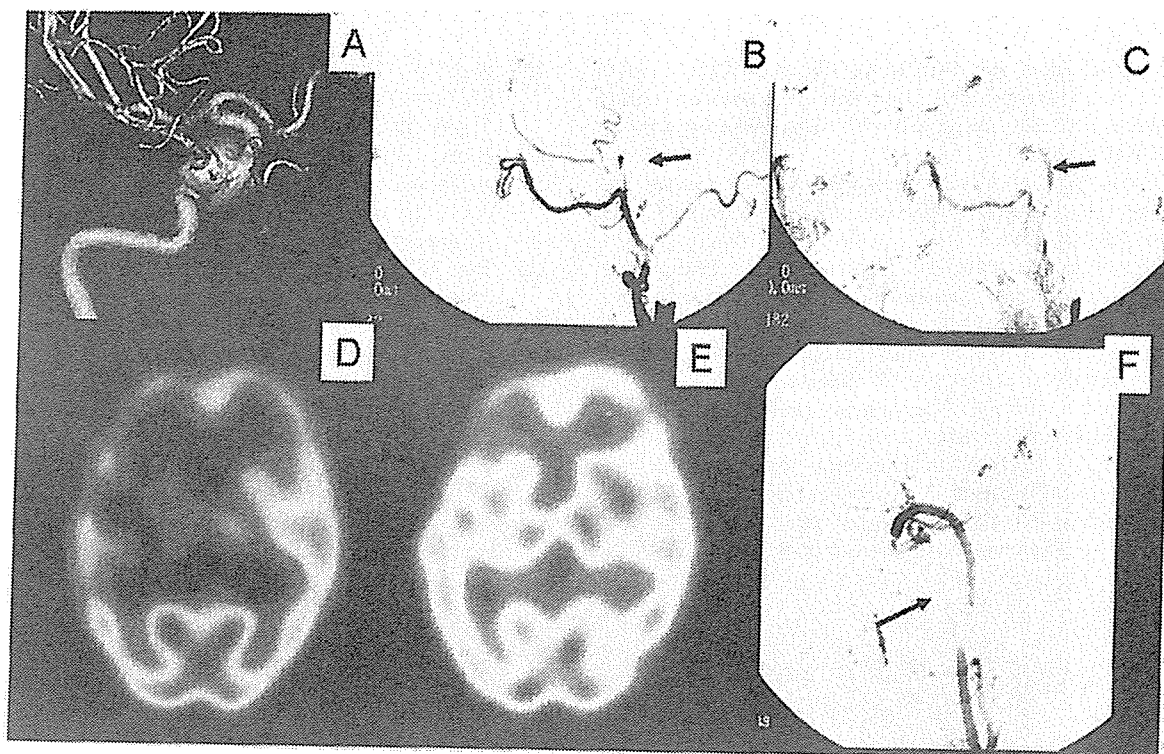


Fig. 3 A 60-year-old woman who complained of diplopia due to right third cranial nerve palsy. A: A 3DDSA showing a large right ICA aneurysm at the cavernous portion. B (early phase) and C (late phase): Right common carotid angiograms during BTO showing opacification of petrous portion ICA (arrows) from branches of external carotid artery. D: An ECD SPECT during BTO of right ICA showing marked flow reduction in the right cerebral hemisphere (residual flow <70% of the contralateral region). E: An IMP SPECT obtained next day of the surgery showing sufficient flow in the right cerebral hemisphere. F: An angiography after surgery of external carotid-right middle cerebral artery bypass using saphenous vein graft and intravascular embolization (arrow) of right ICA just above the collateral flow shown in B and C.

きわめて限定した症例にのみ行うべきと考える。

海綿静脈洞内動脈瘤の場合、通常は頸部内頸動脈の遮断で十分であるが、約20%の症例でpetrous portionにおけるEC-IC間の側副血行がBTOによってのみ判明することがあり、注意が必要と思われる¹⁾¹²⁾。われわれはこの側副血行が存在する場合、その末梢において血管内塞栓によりICOを行っている。

今回はbypass+ICO症例の短期成績について検討したが、今後長期成績や脳血流の面からの詳細な検討を行っていく必要があると思われる。

ま と め

クリッピングも瘤内塞栓も困難な内頸動脈瘤症例において、BTOに基づいてbypass+ICOを行うことにより、良好な短期治療成績が得られた。BTOの安全性向上、ICOに伴う穿通枝障害の回避、長期的な成績の検討、などが今後の課題と思われた。

文 献

- 1) Allen JW, Alastraja AJG, Nelson PK: Proximal intracranial internal carotid artery branches: prevalence and importance for balloon occlusion test. *J Neurosurg* 102: 45-52, 2005
- 2) Field M, Jungreis CA, Chengelis N, *et al*: Symptomatic cavernous sinus aneurysms: management and outcome after carotid occlusion and selective cerebral revascularization. *AJNR* 24: 1200-1207, 2003
- 3) Hongo K, Horiuchi T, Nitta J, *et al*: Double-insurance bypass for internal carotid artery aneurysm surgery. *Neurosurgery* 52: 597-602, 2003
- 4) Houkin K, Kamiyama H, Kuroda S, *et al*: Long-term patency of radial artery graft bypass for reconstruction of the internal carotid artery. Technical note. *J Neurosurg* 90: 786-790, 1999
- 5) 勝間田篤, 杉生憲志, 佐々原渉, ほか: 内頸動脈閉塞試験の合併症—119例の経験から—. *脳神経外科ジャーナル* 13: 572-577, 2004
- 6) Linskey ME, Jungreis CA, Yonas H, *et al*: Stroke risk after abrupt internal carotid artery sacrifice: accuracy of preoperative assessment with balloon test occlusion and stable xenon-enhanced CT. *AJNR* 15: 829-843, 1994

- 7) Marshall RS, Lazar RM, Young WL, *et al*: Clinical utility of quantitative cerebral blood flow measurements during internal carotid artery test occlusions. *Neurosurgery* 50: 996-1004, 2002
- 8) Mathis JM, Barr JD, Jungreis CA, *et al*: Temporary balloon test occlusion of the internal carotid artery. *AJNR* 16: 749-754, 1995
- 9) Ogasawara K, Ogawa A, Yoshimoto T: Cerebrovascular reactivity to acetazolamide and outcome in patients with symptomatic internal carotid or middle cerebral artery occlusion: a xenon-133 single-photon emission computed tomography study. *Stroke* 33: 1857-1862, 2002
- 10) Sekhar LN, Duff JM, Kalavakonda C, *et al*: Cerebral revascularization using radial artery grafts for the treatment of complex intracranial aneurysms: techniques and outcomes for 17 patients. *Neurosurgery* 49: 646-658, 2001
- 11) Serbinenko FA: Balloon catheterization and occlusion of major cerebral vessels. *J Neurosurg* 41: 125-145, 1974
- 12) 清水宏明, 富永悌二, 吉本高志: バイパス併用脳動脈瘤手術における Matas test 特異的な EC-IC 側副血行路. *脳卒中の外科* 31: 269-272, 2003
- 13) Spetzler RF, Schuster H, Roski RA: Elective extracranial-intracranial arterial bypass in the treatment of inoperable giant aneurysms of the internal carotid artery. *J Neurosurg* 53: 22-27, 1980
- 14) Tarr RW, Jungreis CA, Horton JA, *et al*: Complication of preoperative balloon test occlusion of the carotid arteries: experience in 300 cases. *Skull Base Surg* 1: 240-244, 1991
- 15) van Rooji WJ, Sluzewski M, Metz NH, *et al*: Carotid balloon occlusion for large and giant aneurysms: evaluation of a new test occlusion protocol. *Neurosurgery* 47: 116-122, 2000
- 16) Wolf RL, Imbesi SG, Galetta SL, *et al*: Development of a posterior cerebral artery aneurysm subsequent to occlusion of the contralateral internal carotid artery for giant cavernous aneurysm. *Neuroradiology* 44: 443-446, 2002

INTRAOPERATIVE APPLICATION OF THERMOGRAPHY IN EXTRACRANIAL-INTRACRANIAL BYPASS SURGERY

Yoshikazu Okada, M.D., Ph.D.

Department of Neurosurgery,
Tokyo Women's Medical University,
Tokyo, Japan

Takakazu Kawamata, M.D.,
Ph.D.

Department of Neurosurgery,
Tokyo Women's Medical University,
Tokyo, Japan

Akitsugu Kawashima, M.D.,
Ph.D.

Department of Neurosurgery,
Tokyo Women's Medical University,
Tokyo, Japan

Tomokatsu Hori, M.D., Ph.D.

Department of Neurosurgery,
Tokyo Women's Medical University,
Tokyo, Japan

Reprint requests:

Yoshikazu Okada, M.D., Ph.D.,
Department of Neurosurgery,
Tokyo Women's Medical University,
8-1 Kawada-cho, Shinjuku-ku,
Tokyo 162-8666, Japan.
Email: yokada@nij.twmu.ac.jp

Received, June 19, 2006.

Accepted, November 1, 2006.

AQ:1

OBJECTIVE: The extracranial-intracranial bypass may have the potential to improve hemodynamic cerebral ischemia caused by occlusive diseases of the main cerebral arteries. Intraoperative confirmation of effective distribution of blood flow via the donor arteries to the involved region will assure a successful bypass surgery.

METHODS: Infrared thermography was used to measure temperature of the cortical surface at the operative field. Regional cerebral blood flow (rCBF) was measured with a laser Doppler flow meter. Changes in cortical surface temperature before and after temporary occlusion of the bypass were compared with changes in rCBF values at the corresponding sites.

RESULTS: Thermographic examination demonstrated a heterogeneous increase of cortical surface temperature caused by the blood flow via the extracranial-intracranial bypass and was closely related to rCBF changes.

CONCLUSION: Thermography is useful not only to demonstrate the distribution of blood flow through the extracranial-intracranial bypass, but also to quantitatively evaluate the rCBF changes in the operative field.

KEY WORDS: Cerebral ischemia, Extracranial-intracranial bypass, Hemodynamic, Regional cerebral blood flow, Thermography

Neurosurgery 60(ONS Suppl 2):ONS-0-ONS-0, 2007

DOI: 10.1227/01.NEU.0000255358.86947.9A

Thermographic techniques have been developed and applied in many fields, including neurosurgery (6, 7, 11). Of special interest in neurosurgery is thermographic investigation of cortical circulation. Previous experimental studies qualitatively demonstrated a relationship between cortical surface temperature and cerebral blood flow (CBF) after ischemic insults of the brain. Okudera et al. (11) used intraoperative thermographic imaging clinically during surgical resection of a cerebral arteriovenous malformation and demonstrated changes of the surface temperature of the cortical draining vein and the surrounding cortical surface before and after occlusion of the main feeder.

Although extracranial-intracranial (EC-IC) bypass failed to prevent recurrence of stroke (2), some reports have demonstrated the potential effectiveness of superficial temporal artery (STA)-to-middle cerebral artery (MCA) anastomosis to improve compromised hemodynamic cerebral ischemia (8, 9). Consequently, regional

CBF (rCBF) studies are required to identify appropriate candidates for bypass surgery. In addition, intraoperative data of anastomotic blood flow and its distribution are important to confirm an effective EC-IC bypass. Currently, anastomotic flow can be measured intraoperatively by several methods, including the electromagnetic flow meter, Doppler flow meter, visual light spectroscopy, and videoangiography (1, 5, 13). Distribution of anastomotic blood flow can only be detected by rCBF measurement at multiple sites of the operative field using a laser Doppler flow meter and/or thermocouple flow meter.

We have conducted intraoperative thermographic studies with an infrared camera that can be used to quantitatively measure the cortical surface temperature during EC-IC bypass surgery. In this study, cortical surface temperature and rCBF were simultaneously investigated to clarify the relationship between the thermal and rCBF changes caused by the anastomotic blood flow.

PATIENTS AND METHODS

Ten patients were selected for EC-IC bypass surgery based on neurological examination, computed tomographic (CT) scan findings, and rCBF studies. The results of the neurological examination in the 10 patients ranged from transient neurological deficits to minor complete stroke. CT scans showed small (diameter, <2 cm), low-density areas caused by cerebral ischemia. Angiography revealed internal carotid artery (ICA) or MCA occlusive disease. A CBF study of the patients using cold xenon-enhanced CT showed a reduction of more than 20% in rCBF at the affected MCA territory. The Diamox (Wyeth Pharmaceuticals, Collegeville, PA) loading test (17 mg/kg administered intravenously) demonstrated an increase of less than 10% in rCBF at the affected MCA territory compared with the resting CBF.

All patients underwent STA-MCA double anastomoses more than 2 months after their most recent ischemic attack. Frontoparietotemporal craniectomy was performed on the affected side with the patient under general anesthesia. The donor artery was harvested by dissecting the STA. Recipient arteries were selected from the cortical branches of the MCA. In general, we prepared two donor arteries, the frontal and parietal branches of the STA; and two recipient arteries, the supra- and infra-Sylvian cortical branches of the MCA. A silicone stent (diameter, 400 μ m; length, 3–4 mm) that we designed was inserted into the recipient artery through an arteriotomy to facilitate surgical preparation (10). Systemic arterial blood pressure was measured at the radial artery.

Rectal temperature was maintained between 35 and 36°C with a heating pad; room temperature was maintained at 23°C to maintain the background cortical surface temperature as constant as possible. A portable infrared camera (Tversus-100ME model; Nippon Avionics Inc., Tokyo, Japan) and a television monitor were used for intraoperative thermographic examinations. The range of thermographic measurement was from 0 to 50°C, the temperature resolution was 0.1°C, and the scan speed was 10 frames per second. The cortical surface temperatures at three regions of interest (ROIs) were simultaneously displayed in real-time on the monitor. The data were recorded on a 3.5-inch floppy disk and analyzed with thermal measurement computer software (Nippon Avionics Inc.). We determined the changes in cortical surface temperature as a result of the STA-MCA bypass at the completion of the surgical procedures by performing thermographic studies before and after temporary occlusion (20–30 s) of the bypass. We used this method instead of measuring the temperatures before and after the surgical procedure because the cortical temperature before starting the surgical procedure would have been recorded a long time before completion of the bypass procedures and, thus, may not be accurate as the baseline value because of temperature changes during the surgical procedures.

Intraoperative rCBF was measured using a laser Doppler flow meter (ALF 21; Advance Co., Tokyo, Japan) at sites corresponding to the ROIs of thermographic measurement of cortical surface temperature, including at least two sites of the

supra- and infra-Sylvian areas. The effects of STA-MCA bypass on brain surface temperature and rCBF were investigated by temporary occlusion of the bypass, as described above. During the operation, arterial blood gases were monitored to ensure normocapnia and normoxia.

RESULTS

Ten patients underwent operation without any problems and had excellent bypass patency. A representative case of a 70-year-old man with transient right hemiparesis is shown in *Figure 1*. Left ICA occlusion was demonstrated on carotid angiograms. Resting rCBF studies showed a 30% reduction, and 0% vascular reactivity was observed in cold Xe-CBF studies. Cortical surface temperature was measured at five ROIs (*Fig. 2, A and B*). Temporary occlusion of the STA-MCA bypass produced heterogeneous changes in cortical surface temperature of the affected area (*Fig. 2, A–C*). The changes in cortical surface temperature at the ROIs varied from 2 to 0°C. Release of the temporary occlusion of the STA-MCA bypass resulted in prompt recovery of temperature to the preocclusion level at each ROI (*Fig. 2C*). Postoperative examination with magnetic resonance angiography and/or conventional angiography showed excellent patency of the STA-MCA bypass (*Fig. 1B*).

The cortical surface temperature and temperature changes after the bypass procedure were not homogenous but were heterogeneous in all patients studied (*Fig. 2*). Although cortical temperature in some ROIs changed only slightly, all patients showed increased cortical temperature after STA-MCA bypass surgery.

Measurements by laser Doppler flow meter also demonstrated evident changes in rCBF at the sites at which brain surface temperature changed drastically after temporary occlusion of the bypass. The relationship between the change in surface temperature and the corresponding change in rCBF at 20 ROIs was analyzed. A significant correlation was obtained between cortical surface temperature and rCBF changes ($y = 8.9x - 0.8$; $r^2 = 0.656$; $P < 0.0001$) (*Fig. 3*).

DISCUSSION

This study suggests that thermography is useful to monitor changes in cortical circulation caused by EC-IC bypass, indicat-

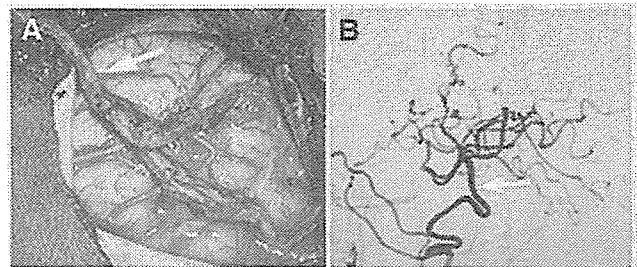


FIGURE 1. A 70-year-old man with left ICA occlusion presented with transient right hemiparesis. A, intraoperative field after STA (arrow)-MCA bypass. B, postoperative angiogram showing excellent patency of STA (arrow)-MCA anastomosis.

THERMOGRAPHY AND EXTRACRANIAL-INTRACRANIAL BYPASS SURGERY

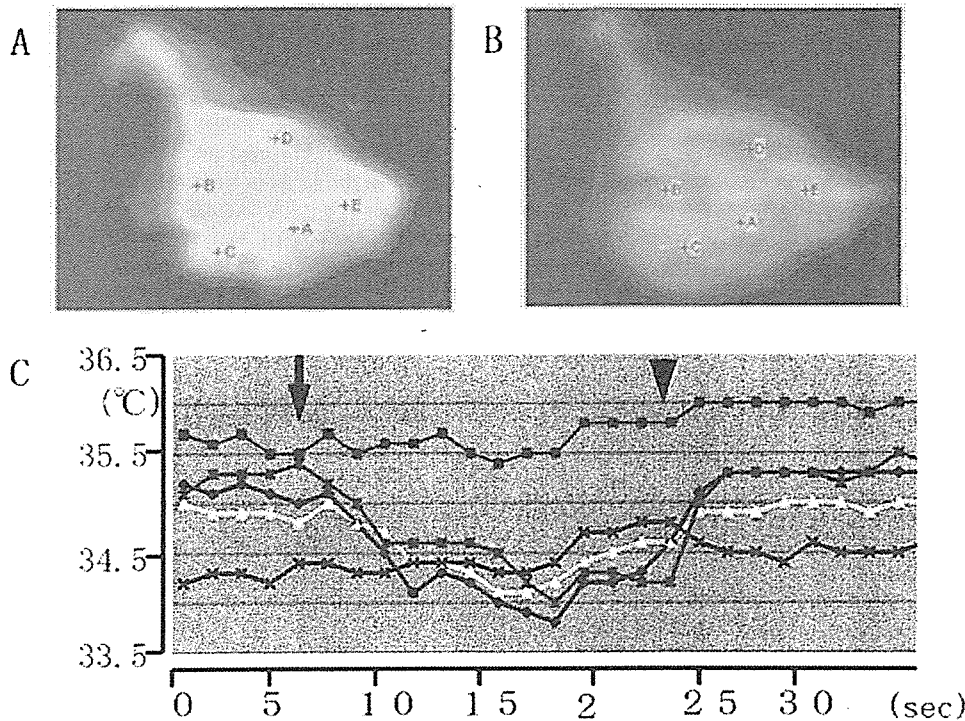


FIGURE 2. Thermographic monitoring of the operative field showing the brain surface temperature before (A) and during (B) occlusion of the anastomosed STA. C, thermography demonstrating heterogeneous changes in cortical surface temperatures measured at five ROIs (+A, +B, +C, +D, +E) with temporary occlusion (area between arrow and arrowhead) of the anastomosed STA.

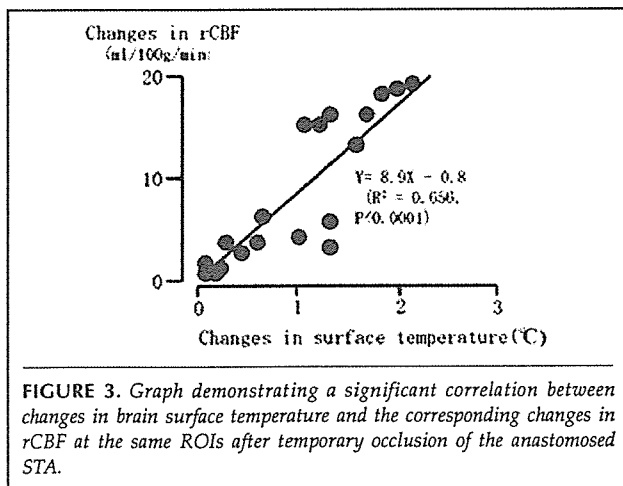


FIGURE 3. Graph demonstrating a significant correlation between changes in brain surface temperature and the corresponding changes in rCBF at the same ROIs after temporary occlusion of the anastomosed STA.

ing not only an increase in regional blood flow, but also the distribution of newly supplied blood.

Infrared thermographic imaging is an established technique for the measurement of the surface temperature of any type of

object. In the past, this method had limited application in the neurosurgical field because of low sensitivity and resolution. However, the latest thermographic systems have rapid response and high sensitivity. Therefore, thermographic equipment is now able to measure local cortical thermal changes resulting from alterations of rCBF because of surgical manipulations. Brock et al. (3) demonstrated local temperature and blood flow changes caused by cortical compression by thermography. Kondo et al. (7) applied thermography to examine the thermal changes and thermal distribution of a free bone flap with drilling and demonstrated prominent temperature elevation at the drilled site, which was reduced by intermittent irrigation with cold water. Further functional activation of somatosensory area was detected as an elevated temperature site using the latest thermographic system (12). However, although

thermography has been used in pathophysiological and technological studies in many fields, to our knowledge, this method has not been applied to evaluate cerebral vascular reconstructive surgeries, the success of which depends on excellent patency and appropriate distribution of blood flow. After the first reports by Donaghy (4) and Yaşargil (14), EC-IC bypass has become an accepted technique to augment CBF in patients with occlusive cerebrovascular disease. Thermographic investigation of EC-IC bypass demonstrates not only bypass patency, but also distribution of the anastomotic blood flow. Furthermore, intraoperative thermographic study of the cortical surface temperature may predict local or diffuse cerebral hyperperfusion after EC-IC bypass surgery. We sometimes experience hyperperfusion, even during and shortly after STA-MCA bypass surgery, particularly in patients with moyamoya disease (unpublished data). To prevent hyperperfusion during postoperative management, it is important to control the patient's blood pressure appropriately, even just after the bypass surgery, on the basis of the intraoperative thermographic findings. Our intraoperative thermographic findings may predict quantitative circulatory changes after bypass surgery. These thermal findings will play an important role in achieving steady and useful cerebral revascularization.

OKADA ET AL.

REFERENCES

1. Amin-Hanjani S, Du X, Mlinarevich N, Meglio G, Zhao M, Charbel FT: The cut flow index: An intraoperative predictor of the success of extracranial-intracranial bypass for occlusive cerebrovascular disease. *Neurosurgery* 56 [Suppl 1]:75–85, 2005.
- AQ:4 2. Anonymous: Failure of extracranial-intracranial arterial bypass to reduce the risk of ischemic stroke. Results of an international randomized trial. The EC/IC Bypass Study Group. *N Engl J Med* 313:1191–1200, 1985.
3. Brock M, Risberg J, Ingvar DH: Effects of local trauma on the cortical cerebral blood flow, studied by infrared thermography. *Brain Res* 12:238–242, 1969.
4. Donaghy RM: Neurologic surgery. *Surg Gynecol Obstet* 134:269–270, 1972.
5. Hoshino T, Katayama Y, Sakatani K, Kano T, Murata Y: Intraoperative monitoring of cerebral blood oxygenation and hemodynamics during extracranial-intracranial bypass surgery by a newly developed visible light spectroscopy system. *Surg Neurol* 65:569–576, 2006.
6. Koga H, Mori K, Ono H, Kuwahara M, Matsuse E: Intraoperative regional thermography during surgery of brain tumors [in Japanese]. *Neurol Med Chir (Tokyo)* 27:1033–1038, 1987.
7. Kondo S, Okada Y, Iseki H, Hori T, Takakura K, Kobayashi A, Nagata H: Thermological study of drilling bone tissue with a high-speed drill. *Neurosurgery* 46:1162–1168, 2000.
8. Nussbaum ES, Erickson DL: Extracranial-intracranial bypass for ischemic cerebrovascular disease refractory to maximal medical therapy. *Neurosurgery* 46:37–43, 2000.
9. Okada Y, Shima T, Nishida M, Yamane K, Yamada T, Yamanaka C: Effectiveness of superficial temporal artery-middle cerebral artery anastomosis in adult moyamoya disease: Cerebral hemodynamics and clinical course in ischemic and hemorrhagic varieties. *Stroke* 29:625–630, 1998.
10. Okada Y, Shima T, Yamane K, Yamanaka C, Kagawa R: Cylindrical or T-shaped silicone rubber stents for microanastomosis—Technical note. *Neurol Med Chir (Tokyo)* 39:55–58, 1999.
11. Okudera H, Kobayashi S, Toriyama T: Intraoperative regional and functional thermography during resection of cerebral arteriovenous malformation. *Neurosurgery* 34:1065–1067, 1994.
12. Ueda M, Sakurai T, Kasai K, Ushikubo Y, Samejima H: Localisation of sensory motor cortex during surgery by changes of cortical surface temperature after median nerve stimulation. *Lancet* 350:561, 1997.
13. Woitzik J, Horn P, Vajkoczy P, Schmiedek P: Intraoperative control of extracranial-intracranial bypass patency by near-infrared indocyanine green videoangiography. *J Neurosurg* 102:692–698, 2005.
14. Yaşargil MG: Anastomosis between the superficial temporal artery and a branch of the middle cerebral artery, in Yaşargil MG (ed): *Microsurgery Applied to Neurosurgery*. Stuttgart, Georg Thieme Verlag, 1969, pp 105–115.

T. Hori
Y. Okada
T. Maruyama
M. Chernov
W. Attia

Endoscope-Controlled Removal of Intrameatal Vestibular Schwannomas

Abstract

The use of endoscopes for surgery of the cerebellopontine angle tumors is steadily obtaining widespread acceptance. The objective of the present study was a laboratory and clinical evaluation of the safety of the endoscope-controlled microneurosurgical removal of the intrameatal vestibular schwannomas through a retrosigmoid approach. The anatomical investigation was done on formalin-fixed cadaver heads and dry temporal bones. Clinical series included 33 consecutive patients (23 women and 10 men; mean age 50 ± 15 years). A bayonet-style rigid endoscope with 70° angle of view and 4 mm outer diameter was found to be optimal for observation of the internal auditory canal. Its insertion in the cerebellopontine cistern should be preferably done under control through an operating microscope. Endoscope-controlled manipulations necessitate the use of a special holder system, which provides a stable position of the device and allows bimanual manipulations by the surgeon. A thermographic evaluation did not reveal a significant increase of the local temperature due to use of the endoscope. Use of the endoscope permitted removal of the neoplasm from the most lateral part of the internal auditory canal and identification of the nerve of tumor origin. In total, 28 tumors underwent total removal, and anatomical preservation of the facial nerve was attained in 31 cases. Damage of the facial nerve by the endoscope was met once. In 8 out of 16 patients, who showed serviceable hearing before surgery, this was preserved after tumor removal. In conclusion, endoscope-controlled removal of the intrameatal vestibular schwannomas seems to be a technically feasible, effective and safe procedure.

Nevertheless, good equipment and special training are absolutely necessary for attainment of optimal results.

Key words

Vestibular schwannoma · endoscope-controlled removal · neuroendoscopy · internal acoustic meatus

Introduction

Complete microneurosurgical excision represents the ideal treatment option for symptomatic patients with vestibular schwannomas [1]. On average 96% of the tumors can be removed totally, which provides the best possible long-term local control [2]. However, the treatment is accompanied by the well-known risk of postoperative complications, such as hearing loss, facial nerve palsy, and cerebrospinal fluid (CSF) leak. Many technical adjuncts were proposed for their prevention. Recently, there has been growing interest in the use of neuroendoscopes during surgery for cerebellopontine angle (CPA) tumors [3–15], because the possibility “to look around the corner” is very attractive for early identification of the cranial nerves and inspection of the internal auditory canal (IAC). However, the efficacy of the technique is not yet completely known. Moreover, there is some concern about possible endoscope-related complications due to poor overview of the operative field, the limited two-dimension-

Department of Neurosurgery, Neurological Institute, Tokyo Women's Medical University, Tokyo, Japan

Affiliation

Correspondence

Prof. Tomokatsu Hori, M. D. · Department of Neurosurgery · Neurological Institute · Tokyo Women's Medical University · 8-1 Kawada-cho · Shinjuku-ku · Tokyo 162-8666 · Japan · Tel.: +81/3/3353-8111 (ext. 26216) · Fax: +81/3/5269-7438 · E-mail: thori@nij.twmu.ac.jp

Bibliography

Minim Invas Neurosurg 2006; 49: 25–29 © Georg Thieme Verlag KG Stuttgart · New York
DOI 10.1055/s-2006-932125
ISSN 0946-7211

al image, and possible local increase of temperature in the vicinity to the tip of the device [10,11,13]. Therefore, we conducted both a laboratory and a clinical study on the safety of the endoscope-controlled removal of the intrameatal vestibular schwannomas.

Materials and Methods

Laboratory investigation

Endoscope-controlled microneurosurgical removal of an intrameatal vestibular schwannoma through a retrosigmoid approach was simulated on 2 formalin-fixed cadaver heads and 2 dry temporal bones. After craniotomy, which was done by a high-speed drill, the rigid bayonet-style endoscope was inserted into the CPA. Commercially available 19-cm and 23-cm long devices with 0°, 30°, and 70° angles of view, and outer diameters of 2.7 and 4 mm were tested consequently. Two sets of observations were done: initially the endoscope connected with videocamera and cold light source was manipulated freehand; thereafter all manipulations were repeated while the device was fixed in the "EndoArm", a specially designed endoscope holder integrated with a video system (Olympus Co., Tokyo, Japan) [16].

After observation of the CPA, the endoscope was removed and drilling of the posterior wall of the IAC was done with its further inspection by various types of endoscopes, which were manipulated either freehand or were fixed in the "EndoArm" (Fig.1). During observation of the CPA, opening of the IAC by a high-speed drill, and its endoscopic inspection the thermographic study were performed using a portable infrared camera TVS 100 ME (Nippon Avionics Inc., Tokyo, Japan).

Clinical study

During 2004 and 2005, 33 consecutive patients underwent endoscope-controlled microneurosurgical removal of intrameatal vestibular schwannomas at the Department of Neurosurgery of the Tokyo Women's Medical University. There were 23 women and 10 men; mean age constituted 50 ± 15 years. The tumor was located on the left side in 16 cases, and on the right side in 17. There were 31 initially diagnosed and 2 recurrent neoplasms. Three schwannomas were purely intrameatal, 8 had limited extension into the CPA, 7 filled the CPA completely, but did not show compression of the brain stem, and 15 caused more or less prominent brain stem compression. Before surgery 31 patients had either normal, or nearly normal facial nerve function (House-Brackmann grade 1–2 [17]), and 16 patients had functionally preserved hearing (Gardner-Robertson class I-II [18]).

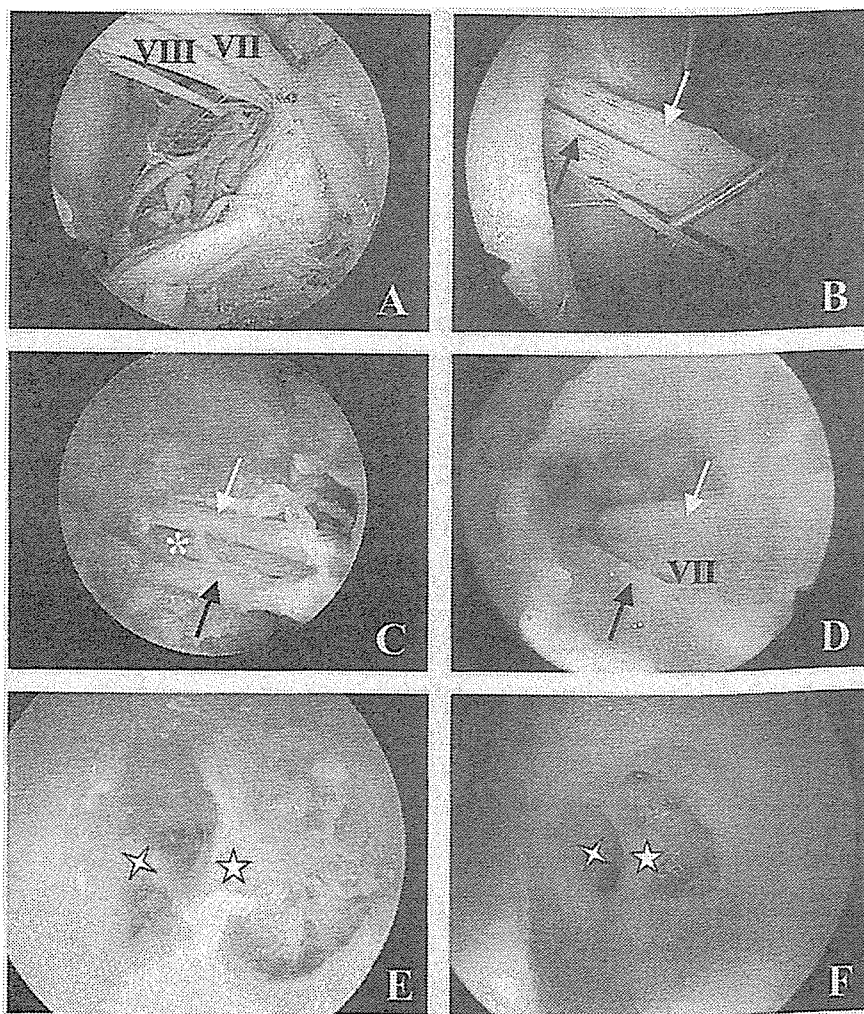


Fig. 1 Neuroendoscopic view of the right CPA during anatomic dissection: identification of origin of the VII and VIII cranial nerves from the brain stem (A), observation of the cisternal portion of the nerves (B), observation of the nerves after removal of the posterior wall of the IAC (C), observation of the most lateral part of the IAC (D), identification of the Bill's bar and transverse crest after removal of the nerves (E) and complete removal of the soft tissues (F). Marked: facial nerve (VII), vestibulocochlear nerve (VIII), superior vestibular nerve (black arrow), inferior vestibular nerve (white arrow), cochlear nerve (asterisk), Bill's bar (crest), and transverse crest (star).

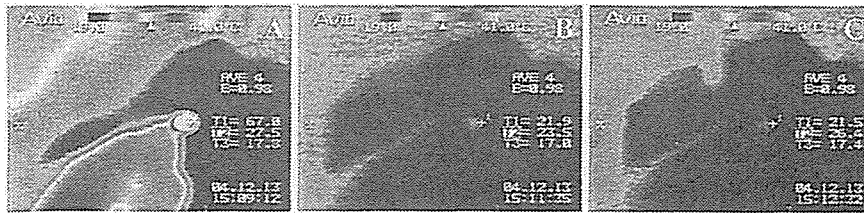


Fig. 2 Thermographic study during simulated endoscope-controlled procedure for intrameatal tumor: the local temperature dramatically increased during drilling of the posterior wall of the IAC (A), but normalized thereafter (B), and did not changed significantly during the use of endoscope (C).

All procedures were planned as routine microneurosurgical operations, so if necessary these could be completed without the use of endoscope. General anesthesia, lateral oblique position of the patient, standard retrosigmoid approach, motor and somatosensory evoked potentials, auditory brain response, facial nerve monitoring, and cochlear nerve action potentials were used routinely, in the same way as described elsewhere [13,14,19,20]. After microsurgical intracapsular debulking of the tumor in the CPA, the posterior wall of the IAC was removed by a high-speed drill. A rigid endoscope fixed in the "EndoArm" was inserted into the CPA under control through an operating microscope. Subsequent removal of the residual tumor from the CPA and IAC was attained utilizing concurrently both microscope- and endoscope-controlled techniques with the use of routine microneurosurgical instruments. Regular irrigation of the wound by Ringer's lactate solution was done during use of the endoscope.

Results

Laboratory investigation

The endoscopes with 0°, 30°, and 70° angles of view were found to be equally useful for observation of the CPA through the retrosigmoid approach. Inspection of the IAC seemed to be optimal using the endoscope with a 70° angle of view and outer diameter 4 mm. The insertion of this device into the CPA and its positioning for visualization of the IAC were found to be difficult without microscopic control. Both freehand fixation of the endoscope and use of the "EndoArm" seemed to be equally suitable for inspection of the CPA and IAC. However, endoscope-controlled microsurgical manipulations could not be effectively done without use of the endoscope-holder system, which provided a stable position of the device and allowed bimanual manipulations by the surgeon. During drilling of the posterior wall of the IAC a thermographic study revealed a prominent increase of the local temperature. Alternatively, the presence of an endoscope connected with a working cold light source in the CPA did not lead to significant changes of the local temperature (Fig. 2).

Clinical study

Use of the endoscope permitted removal of residual tumor from the most lateral part of the IAC (Fig. 3). In all, total tumor removal was done in 28 cases, subtotal removal in 3, and partial removal in 2 cases. Anatomic preservation of the facial nerve was attained in 31 cases. In one case the facial nerve was mechanically damaged by the endoscope itself, which necessitated its direct suturing in the CPA. In 8 out of 16 patients, who showed serviceable hearing preoperatively, this was preserved after tumor removal. No one case of thermal injury to the cranial nerves, postoperative CSF leak, or infection was observed. Histological examination re-

vealed typical schwannomas in all cases; mean MIB-1 index constituted $2.3 \pm 1.9\%$.

Final endoscopic inspection at the end of the procedure gives us an opportunity to define the nerve of tumor origin, either definitely (in 18 cases), or most probably (in 14 cases). Schwannomas arising from the superior vestibular and inferior vestibular nerves were represented in 16 cases each (Figs. 4 and 5). In one case with partial tumor removal the nerve of tumor origin was not defined. Its identification was found to be easier if dilatation of the fundus of the IAC due to tumor growth was present. Meanwhile, no associations were found between the nerve of tumor origin and age and gender of the patient, side and MIB-1 index of the neoplasm, and the presence of useful hearing before surgery.

Discussion

Modern neuroendoscopic devices, both rigid and flexible, provide a wide angle of view, superb illumination with a cold light, and perfect depth of focus in combination with high magnification. Their use during microsurgical procedures allows to reduce the size of the craniotomy, to improve visualization in the operative field, and to look around important anatomic structures, thus eliminating the need for extensive retraction [4,6,11–13,21–23]. Furthermore, the development of "virtual endoscopy" [24,25], which permits to simulate the surgical procedures preoperatively, based on the data of neuroimaging, can significantly increase the clinical efficacy of the technique in the future.



Fig.3 Endoscope-controlled removal of the intrameatal vestibular schwannoma from the lateral part of the IAC.

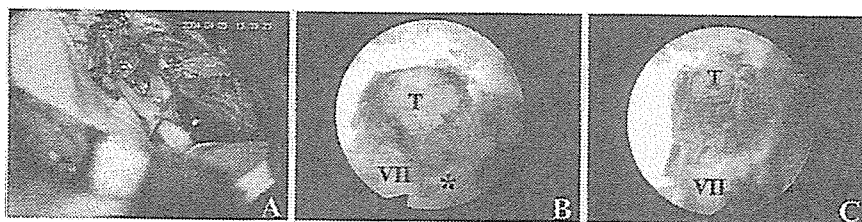


Fig. 4 Endoscope-controlled microneurosurgical removal of the right-sided vestibular schwannoma: view of the tumor in the IAC after removal of its posterior wall (A) and observation of the neoplasm originated from the superior vestibular nerve in the most lateral part of IAC (B and C). Marked: facial nerve (VII), cochlear nerve (asterisk), and tumor (T).

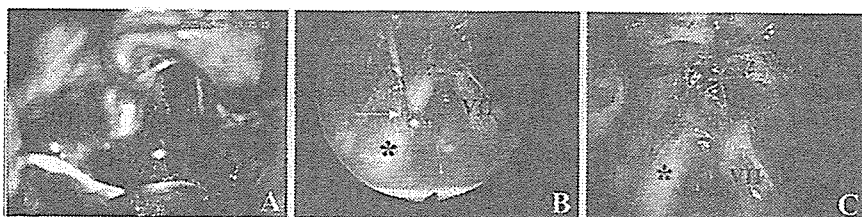


Fig. 5 Endoscope-controlled microneurosurgical removal of the left-sided vestibular schwannoma: view of the tumor after removal of the posterior wall of the IAC (A) and endoscopic observation of the neoplasm originated from the inferior vestibular nerve in the most lateral part of the IAC (B and C). Marked: facial nerve (VII), cochlear nerve (asterisk), tumor (T), and electrode for cochlear nerve action potentials (white arrow).

The advantages of the endoscopic inspection during microsurgical removal of vestibular schwannomas had been highlighted in several previous reports [3–15]. These mainly include early identification of the cranial nerves in the CPA, possibility of revision of the most lateral part of the IAC for the presence of the residual neoplasm, and visualization of the non-sealed petrous bone air cells for prevention of postoperative CSF leak. With the adjunct of endoscopy, tumors can be removed more completely, with less morbidity, and the degree of their resection can be assessed more precisely [3, 7, 10, 13, 23]. The length of drilling of the posterior wall of the IAC can be reduced, and inadvertent opening of the intraosseous endolymphatic sac and posterior semicircular canal, which has a crucial importance in hearing-preservation vestibular schwannoma surgery, can be avoided [9–12]. The technique may be useful for identification of the source of problematic bleeding during removal of the neoplasm [15]. Finally, as was shown in the present series, use of the endoscope permits an exact delineation of the nerve of tumor origin.

While endoscopic inspection during surgery for vestibular schwannomas has obtained widespread acceptance, the advantages of endoscope-controlled removal of these tumors are less clear. Wackym et al. [13] and Magnan et al. [14] advocated use of this technique for the dissection of the residual neoplasm from the most lateral part of the IAC. Goksu et al. [10] reported the results of such procedures in 8 patients with serviceable hearing and small intrameatal vestibular schwannomas: total removal, functional preservation of the facial nerve, and anatomic preservation of the cochlear nerve was attained in all cases, whereas useful hearing was preserved in four cases. In the present series, which included a significant proportion of large tumors, total removal of the neoplasm was attained in 85% of the cases, anatomic preservation of the facial nerve in 94% of cases, and preservation of the serviceable hearing in 50% of those, who showed its presence before surgery.

Our clinical results confirm that integration of endoscope-controlled removal of the intrameatal part of the tumor into micro-neurosurgical excision of vestibular schwannomas is technically

feasible, effective, and safe. Nevertheless, several lessons have been learnt. First, use of rigid endoscopes, which are usually recommended for endoscope-assisted skull base surgery [6, 21, 23], may be complicated during endoscope-controlled procedures due to nearly coaxial positions of the endoscopic device and microinstruments. This disadvantage can be overcome if bayonet-style endoscopes and microinstruments are used. Second, several endoscopes should be available during surgery and used according to the particular goals. While 0°, 30°, and 70° angles of view endoscopes were found to be useful for manipulations in the CPA, only the latter device was suitable for observation of the IAC. Third, angled rigid endoscopes may be difficult to pass in the operative wound without risk of inadvertent damage to the neurovascular structures [5, 6, 23]. Mechanical injury of the facial nerve by the endoscope was met once in the present series. Therefore, we strongly recommend microscopic guidance during insertion of the 70° angle of view device into the CPA.

There is known concern that prolonged use of endoscope can be accompanied by an increase of the local temperature in the vicinity to its tip followed by thermal injury to critical neurovascular structures [11, 13]. This was not, however, confirmed by the conducted laboratory thermographic study. In fact, it was found that local temperature in the CPA during the use of an endoscope connected with a working light source, is much lower, compared with those during removal of the posterior wall of the IAC by a high-speed drill. Moreover, in no one case of our clinical series the thermal injury to the cranial nerves was marked. Definitely, the possibility of this complication may depend on the model of the device, duration of its use, type of light source, and individual sensitivity of the cranial nerves. However, in general, the risk of thermal injury during use of the endoscope should not be considered too high, and regular irrigation of the wound by Ringer's lactate solution seems to serve as a sufficient preventive measure.

Intracranial neuroendoscopic procedures are usually performed through a narrow corridor in the vicinity to important neurovascular structures. While endoscopic inspection can be done by

freehand fixation of the device, endoscope-controlled micro-neurosurgical manipulations require its precise position, because monomanual surgical manipulations may be not only non-effective, but even dangerous if an occasional shift of the endoscope occurs in the surgical wound [5,9–11,13,21–23]. This necessitates the use of special holder, which can provide a stable position of the device in the surgical wound and permits bimanual manipulations by the surgeon and assistant. Several such systems are currently available. One of these is the “EndoArm”, which was used in the present study, and can be suitable for endoscopic inspection, endoscope-assisted, and endoscope-controlled microneurosurgery. It provides excellent maneuverability within 6 degrees of freedom, smooth manipulations with avoidance of strenuous maneuvers of the surgeon, accurate fixation in any direction, and safe release, which result in a high level of clinical safety of the device [16].

Conclusion

Endoscopic inspection during surgery for vestibular schwannomas allows early identification of the cranial nerves, revision of the most lateral part of the IAC for presence of the residual neoplasm, delineation of the nerve of its origin, and visualization of the non-sealed petrous bone air cells for prevention of post-operative CSF leak. Endoscope-controlled microneurosurgical removal of the intrameatal tumors is technically feasible, effective, and safe, and permits to attain dissection of the neoplasm from the most lateral part of the IAC. The risk of thermal injury to the cranial nerves due to use of endoscopes seems to be low. Nevertheless, special training is absolutely necessary, because endoscopic procedures are accompanied by definite learning curve. Availability of good equipment, including an endoscope-holder system, is also very important for attainment of optimal surgical results.

References

- Chernov M, DeMonte F. Skull base tumors. In: Levin VA (ed). *Cancer in the nervous system*, 2nd edn. Oxford: Oxford University Press, 2002: 300–319
- Yamakami I, Uchino Y, Kobayashi E, Yamaura A. Conservative management, gamma-knife radiosurgery, and microsurgery for acoustic neuromas: a systematic review of outcome and risk of three therapeutic options. *Neurol Res* 2003; 25: 682–690
- McKenna KX. Endoscopy of the internal auditory canal during hearing conservation acoustic tumor surgery. *Am J Otol* 1993; 14: 259–262
- Magnan J, Chays A, Lepetre C, Pencroff E, Locatelli P. Surgical perspectives of endoscopy of the cerebellopontine angle. *Am J Otol* 1994; 15: 366–370
- Rosenberg SI, Silverstein H, Willcox TO, Gordon MA. Endoscopy in otology and neurootology. *Am J Otol* 1994; 15: 168–172
- Matula C, Tschabitscher M, Diaz Day J, Reinprecht A, Koos WT. Endoscopically assisted microneurosurgery. *Acta Neurochir (Wien)* 1995; 134: 190–195
- Tatagiba M, Matthies C, Samii M. Microendoscopy of the internal auditory canal in vestibular schwannoma surgery: technique application. *Neurosurgery* 1996; 38: 737–740
- Valtonen HJ, Poe DS, Heilman CB, Tarlov EC. Endoscopically assisted prevention of cerebrospinal fluid leak in suboccipital acoustic neuroma surgery. *Am J Otol* 1997; 18: 381–385
- Jennings CR, O'Donoghue GM. Posterior fossa endoscopy. *J Laryngol Otol* 1998; 112: 227–229
- Goksu N, Bayazit Y, Kemaloglu Y. Endoscopy of the posterior fossa and dissection of acoustic neuroma. *J Neurosurg* 1999; 91: 776–780
- King WA, Wackym PA. Endoscope-assisted surgery for acoustic neuromas (vestibular schwannomas): early experience using the rigid Hopkins telescope. *Neurosurgery* 1999; 44: 1095–1102
- Low WK. Enhancing hearing preservation in endoscopic-assisted excision of acoustic neuroma via the retrosigmoid approach. *J Laryngol Otol* 1999; 113: 973–977
- Wackym PA, King WA, Poe DS, Meyer GA, Ojemann RG, Barker FG, Walsh PR, Staecker H. Adjunctive use of endoscopy during acoustic neuroma surgery. *Laryngoscope* 1999; 109: 1193–1201
- Magnan J, Barbieri M, Mora R, Murphy S, Meller R, Bruzzo M, Chays A. Retrosigmoid approach for small and medium-sized acoustic neuromas. *Otol Neurotol* 2002; 23: 141–145
- Gerganov VM, Romansky KV, Bussarsky VA, Noutchev LT, Iliev IN. Endoscope-assisted microsurgery of large vestibular schwannomas. *Minim Invas Neurosurg* 2005; 48: 39–43
- Morita A, Okada Y, Kitano M, Hori T, Taneda M, Kirino T. Development of hybrid integrated endoscope-holder system for endoscopic microneurosurgery. *Neurosurgery* 2004; 55: 926–932
- House WF, Brackmann DE. Facial nerve grading system. *Otolaryngol Head Neck Surg* 1985; 93: 184–193
- Gardner G, Robertson JH. Hearing preservation in unilateral acoustic neuroma surgery. *Ann Otol Rhinol Laryngol* 1988; 97: 55–66
- Ojemann RG. Retrosigmoid approach to acoustic neuroma (vestibular schwannoma). *Neurosurgery* 2001; 48: 553–558
- Ciric I, Zhao J-C, Rosenblatt S, Wiet R, O'Shaughnessy B. Suboccipital retrosigmoid approach for removal of vestibular schwannomas: facial nerve function and hearing preservation. *Neurosurgery* 2005; 56: 560–570
- Perneczky A, Fries G. Endoscope-assisted brain surgery: Part 1 – evolution, basic concept, and current technique. *Neurosurgery* 1998; 42: 219–225
- Fries G, Perneczky A. Endoscope-assisted brain surgery: Part 2 – analysis of 380 procedures. *Neurosurgery* 1998; 42: 226–232
- Teo C. Endoscopic-assisted tumor and neurovascular procedures. *Clin Neurosurg* 2000; 46: 515–525
- Boor S, Maurer J, Mann W, Stoeter P. Virtual endoscopy of the inner ear and the auditory canal. *Neuroradiology* 2000; 42: 543–547
- Vrabec JT, Briggs RD, Rodriguez SC, Johnson Jr RF. Evaluation of the internal auditory canal with virtual endoscopy. *Otolaryngol Head Neck Surg* 2002; 127: 145–152

Cerebral Oxygen Metabolism and Neuronal Integrity in Patients With Impaired Vasoreactivity Attributable to Occlusive Carotid Artery Disease

Satoshi Kuroda, MD, PhD; Tohru Shiga, MD, PhD; Kiyohiro Houkin, MD, PhD;
Tatsuya Ishikawa, MD, PhD; Chietsugu Katoh, MD, PhD;
Nagara Tamaki, MD, PhD; Yoshinobu Iwasaki, MD, PhD

Background and Purpose—It is still unclear that impaired cerebrovascular reactivity (CVR) to acetazolamide is comparable to elevated oxygen extraction fraction (OEF) on positron emission tomography (PET) in patients with occlusive carotid diseases. Therefore, in this study, the authors aimed to clarify whether OEF is elevated in all patients with reduced cerebral blood flow (CBF) and CVR (type 3) on single photon emission computed tomography (SPECT), and, if not, to specify the underlying pathophysiology of type 3 but normal OEF.

Methods—This study included 46 patients who had decreased CBF and CVR on *N*-isopropyl- p - ^{123}I -iodoamphetamine SPECT in the ipsilateral middle cerebral artery area attributable to occlusive carotid diseases. Hemodynamic and metabolism parameters were determined in all patients by ^{15}O -gas PET, and neuronal integrity was evaluated in 19 patients using ^{11}C -flumazenil (FMZ) PET.

Results—OEF was significantly elevated in 20 (43.5%) of 46 type 3 patients. Another 26 type 3 patients had normal OEF. Regression analysis showed that OEF significantly correlated with cerebral metabolic rate for oxygen and ^{11}C -FMZ binding potential but not with other parameters. Subcortical infarction had no significant effect on OEF values.

Conclusions—The results strongly suggest that type 3 patients with reduced CBF and CVR may be divided into 2 pathophysiologically different subgroups: misery perfusion attributable to hemodynamic compromise and matched hypometabolism attributable to incomplete infarction. Type 3 but normal OEF may represent a transition stage from misery perfusion to matched hypometabolism. (*Stroke*. 2006;37:393-398.)

Key Words: acetazolamide ■ cerebral ischemia ■ flumazenil ■ metabolism ■ oxygen

There is increasing evidence that hemodynamically compromised patients with internal carotid artery (ICA) occlusion are at higher risk for subsequent ischemic stroke. Over these 20 years, an elevated oxygen extraction fraction (OEF) determined by positron emission tomography (PET) has been believed to represent critical reduction of cerebral perfusion pressure, named as “misery perfusion” or “stage II.”^{1,2} Recent statistical analyses have proven that an elevated OEF can be an independent risk factor for subsequent ischemic stroke in patients with occlusive carotid artery disease.^{3–5}

Alternatively, cerebrovascular reactivity (CVR) to CO_2 or acetazolamide has also been used to assess cerebral perfusion reserve in patients with occlusive carotid diseases because single photon emission computed tomography (SPECT) or cold xenon computed tomography (CT) is more widely available and can be done at lower costs than PET. Recent studies have proven that quantitative measurements of cerebral blood flow (CBF) and CVR can also be a predictor for

subsequent ischemic stroke in patients with ICA or middle cerebral artery (MCA) occlusion. Thus, Kuroda et al (2001) reported that relative risk conferred by reduced CBF and CVR (type 3) was 8.0 (95% CI, 1.9 to 34.4) for ipsilateral stroke.⁶ Subsequently, Ogasawara et al also reported similar results.⁷ Based on these observations, SPECT has been expected to identify misery perfusion or stage II more easily than PET if CVR is comparable to OEF.⁸

However, it is still controversial whether impaired CVR is directly linked to OEF elevation in patients with occlusive carotid artery diseases or not. Thus, previous studies have reported a significant correlation between OEF and CVR to acetazolamide or CO_2 .^{9–14} However, the number of patients included in these studies was not so large, and their hemodynamic and metabolic parameters varied widely among the subjects. On the other hand, recent study has shown that $\approx 40\%$ of patients with reduced CVR have normal OEF when both parameters are evaluated in each patient.¹⁵ The issue is

Received September 29, 2005; final revision received November 8, 2005; accepted November 13, 2005.

From the Departments of Neurosurgery (S.K., T.I., Y.I.) and Nuclear Medicine (T.S., C.K., N.T.), Hokkaido University Graduate School of Medicine, Japan; and Department of Neurosurgery (K.H.), Sapporo Medical University, Japan.

Correspondence to Satoshi Kuroda, MD, PhD, Department of Neurosurgery, Hokkaido University Graduate School of Medicine, North 15 West 7, Kita-ku, Sapporo 060-8638, Japan. E-mail skuroda@med.hokudai.ac.jp

© 2006 American Heart Association, Inc.

Stroke is available at <http://www.strokeaha.org>

DOI: 10.1161/01.STR.0000198878.66000.4e

quite important because there may be a significant difference in sensitivity for detecting the patients at higher risk for subsequent stroke between CVR and OEF.

On the other hand, ^{11}C -flumazenil (FMZ) PET has been accepted as a noninvasive, variable tool to investigate neuronal integrity because FMZ is a specific ligand to the central type of benzodiazepine receptors that are exclusively localized in the neurons. Recent studies have shown that ^{11}C -FMZ PET can detect ischemia-induced selective neuronal necrosis that is not visible on either CT or MRI.^{16,17}

Therefore, in this study, the authors aimed to clarify whether OEF is elevated in all patients who are diagnosed as type 3 on SPECT, and, if not, to specify the underlying pathophysiology of normal OEF in spite of type 3. For this purpose, the authors measured the parameters for oxygen metabolism and for neuronal integrity in type 3 patients with occlusive, using ^{15}O -gas and ^{11}C -FMZ PET, respectively.

Subjects and Methods

Patients

The present study included a total of 46 patients who were admitted to our hospital between January 1999 and December 2004. All of them met the following criteria: (1) severe stenosis (>90%) or occlusion of the ipsilateral ICA or MCA; (2) no or, if any, small infarction on MRI; and (3) reduced CBF and CVR to acetazolamide in the ipsilateral MCA territory on [^{123}I]-*N*-isopropyl-*p*-iodoamphetamine (^{123}I -IMP) SPECT (see below). There were 36 men and 10 women with a mean age of 68.2 years (range 48 to 79 years). Their clinical symptoms included transient ischemic attack or amaurosis fugax in 18 patients and minor completed stroke (Rankin score 1 or 2) in 25. The other 3 patients were asymptomatic. Digital subtraction angiography showed ICA occlusion in 27 patients, ICA severe stenosis in 8, MCA occlusion in 5, and MCA severe stenosis in 6. All studies were performed ≥ 4 weeks after the last ischemic episode because the studies in an earlier period might affect the correct interpretation of the data.¹⁸

SPECT Measurements

All patients were scanned with a triple-head γ camera (GCA-9300/DI; Toshiba) to determine CBF and CVR to acetazolamide, as described previously.¹⁶ Briefly, quantitative blood flow was determined by using the ^{123}I -IMP injection and single-scan autoradiographic technique. CBF was quantitatively measured before and 15 minutes after intravenous injection of 10 mg/kg acetazolamide on the separate days with an interval of 2 to 3 days. To evaluate cerebral hemodynamics, 10-mm diameter circular regions of interest (ROIs) were symmetrically placed in the ipsilateral and contralateral MCA territories. As described previously,^{6,18,19} CVR to acetazolamide was quantitatively calculated as: $\text{CVR} (\%) = 100 \times (\text{CBF}_{\text{ACZ}} - \text{CBF}_{\text{rest}}) / \text{CBF}_{\text{rest}}$, where CBF_{rest} and CBF_{ACZ} represent CBF before and after intravenous injection of acetazolamide, respectively. Normal control values of CBF (mean \pm SD = 38.1 ± 5.4 mL/min per 100 g) and CVR ($30.0 \pm 8.0\%$) in

the MCA territory were obtained from 10 normal volunteers free of cerebrovascular disease. The values were rated as reduced when any of them were less than mean -2 SD. Thus, in the current study, patients were judged as type 3 when CBF was <27 mL/min per 100 g and CVR was $<14\%$.¹⁶

PET Measurements

All patients were scanned with ECAT EXACT HR+ (Siemens) as described previously.¹⁶ The intervals between SPECT and PET measurements were within 2 weeks. One-minute inhalation of ^{15}O -CO (2 GBq/min) followed by 3-minute static scanning and 3-time arterial blood sampling were performed to measure cerebral blood volume (CBV). After 15-minute inhalation of ^{15}O -O₂ (0.5 GBq/min), a steady-state O₂ image was scanned and 3-time arterial blood sampling was performed for 5 minutes to measure OEF and cerebral metabolic rate for oxygen (CMRO₂). Finally, to determine CBF, steady-state CO₂ image was scanned and 3-time arterial blood sampling was performed for 5 minutes after 15-minute inhalation of ^{15}O -CO₂ (0.5 GBq/min). Normal PET values were obtained from 10 volunteers: CBF, 44 ± 4 mL/min per 100 g; CMRO₂, 3.3 ± 0.6 mL/min per 100 g; CBV, 3.7 ± 0.7 mL/min, and OEF, 0.43 ± 0.05 (mean \pm SD). Each PET parameter was obtained using 10-mm diameter circular ROIs. The values were rated as decreased when any of them were less than mean -2 SD and rated as increased when any of them were more than mean $+2$ SD.

The dynamic FMZ PET was studied in 19 of 46 patients at the same time that ^{15}O -gas PET was performed, as reported previously.¹⁶ Briefly, the injected dose of ^{11}C -FMZ was 370 MBq for each patient. The binding potential (BP) images were calculated pixel by pixel using the reference tissue model.²⁰

Data Analysis

To evaluate various parameters obtained from ^{123}I -IMP SPECT, ^{15}O -gas PET, and ^{11}C -FMZ PET, the SPECT and PET images were automatically coregistered to axial T1-weighted MRI images. The SPECT, PET, and MRI images were registered using fully automatic multimodality image registration algorithm on Unix-based workstation (Indigo 2; SGI Inc.).²¹

All data were expressed as mean \pm SD. The data between 2 groups were compared by use of χ^2 test or paired t test as appropriate. Differences with a P value of <0.05 were considered statistically significant.

Results

^{15}O PET Parameters

CBF, CBV, CMRO₂, and OEF in type 3 patients are shown in the Table. There were significant differences in CBF, CMRO₂, and OEF between the ipsilateral and contralateral MCA areas. However, there was no significant difference in CBV between them.

Relationships between OEF and other PET parameters were analyzed in the ipsilateral hemispheres (Figure 1). There was no significant correlation between OEF and CBF ($R^2=0.001$;

Quantitative Data of Hemodynamic and Metabolic Parameters in the Ipsilateral and Contralateral MCA Areas in Type 3 Patients

	Type 3 Patients			Control Value
	Ipsilateral MCA Area	Contralateral MCA Area	Significance	
n	46	46		10
CBF, mL/100 g/min	24.8 ± 4.5	31.9 ± 6.3	$P < 0.0001$	44.0 ± 4.0
CBV, mL/100 g	4.2 ± 1.1	3.8 ± 1.1	NS	3.70 ± 0.70
CMRO ₂ , mL/100 g/min	1.98 ± 0.48	2.27 ± 0.48	$P = 0.0045$	3.30 ± 0.60
OEF	0.46 ± 0.09	0.40 ± 0.05	$P < 0.0001$	0.43 ± 0.05

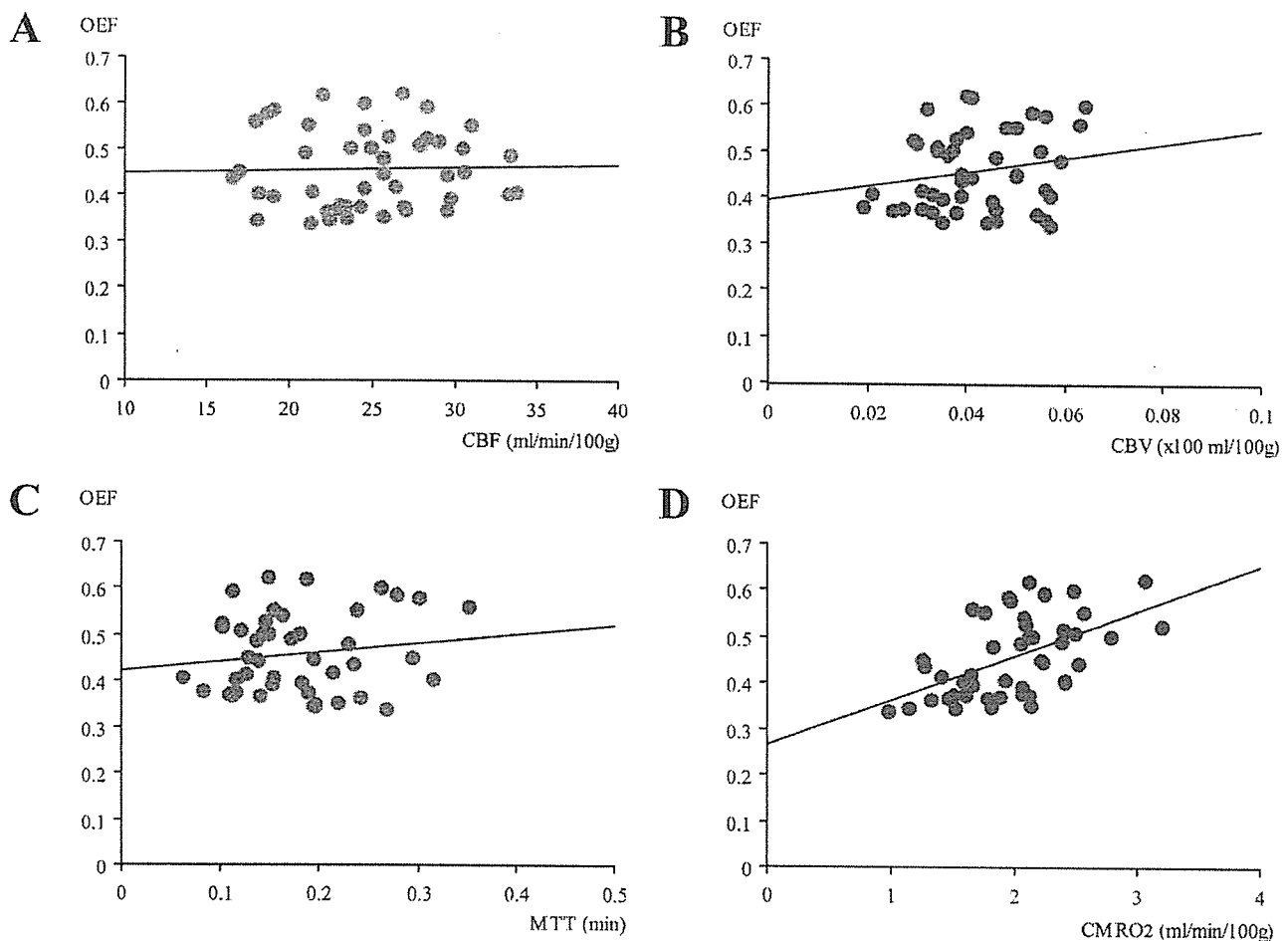


Figure 1. Regression analysis of the relationships between OEF and CBF (A), CBV (B), MTT (C), or CMRO₂ (D) in 46 type 3 patients.

$P=0.841$), between OEF and CBV ($R^2=0.041$; $P=0.1794$), or between OEF and mean transit time (MTT; $R^2=0.023$; $P=0.3169$). On the other hand, there was significant, positive correlation between OEF and CMRO₂ ($R^2=0.081$; $P=0.006$).

Then the values of OEF, CMRO₂, and CBV were evaluated in each patient. Although OEF was significantly higher in the ipsilateral MCA area than in the contralateral side, OEF was significantly elevated in only 20 (43.5%) of 46 patients. OEF was kept within normal limits in the other 26 patients (Figure 2).

CMRO₂ was significantly higher in patients with elevated OEF than in those with normal OEF: 2.26 ± 0.41 and 1.78 ± 0.42 mL/100 g per minute, respectively ($P=0.0002$; Figure 3). Of 20 patients with elevated OEF, 14 (70%) had normal CMRO₂ and the other 6 (30%) had decreased CMRO₂ (<2.1 mL/100 g per minute). On the other hand, of 26 patients with normal OEF, 7 (26.9%) had normal CMRO₂ and the other 19 (73.1%) had decreased CMRO₂. Thus, normal CMRO₂ was more frequently observed in patients with elevated OEF than in those with normal OEF ($P=0.0032$; Figure 3).

There was no significant difference in CBV between patients with elevated OEF and with normal OEF: 4.4 ± 1.1 and 4.0 ± 1.1 mL/100 g, respectively ($P=0.2357$; Figure 3). However, of 20 patients with elevated OEF, 9 (45%) had increased CBV. Of 26 patients with normal OEF, only 4

(15.4%) had increased CBV. As the result, increased CBV was more frequently denoted in patients with elevated OEF than in those with normal OEF ($P=0.0264$; Figure 3).

^{11}C -FMZ Binding Potential

To evaluate the neuronal integrity in patients with type 3 ischemia, ^{11}C -FMZ PET was performed in 19 (41.3%) of 46 patients. The relationships between the ratio of the ipsilateral to contralateral ^{11}C -FMZ BP and metabolic parameters were analyzed. There was a significant, positive correlation between the ratio and OEF ($R^2=0.507$; $P=0.0006$; Figure 4). The ratio also significantly correlated with CMRO₂ ($R^2=0.324$; $P=0.011$).

MRI

Using T2-weighted MRI, the localization of cerebral infarction was evaluated to clarify its effects on cerebral oxygen metabolism and neuronal integrity. Subcortical infarction in the ipsilateral hemisphere was found in 7 of 20 patients with elevated OEF and in 16 of 26 patients with normal OEF. There was no significant effect of subcortical infarction on OEF value in type 3 patients (χ^2 test $P=0.0743$).

Discussion

The present results revealed that hemodynamic and metabolic parameters in type 3 patients are not uniform, and that they

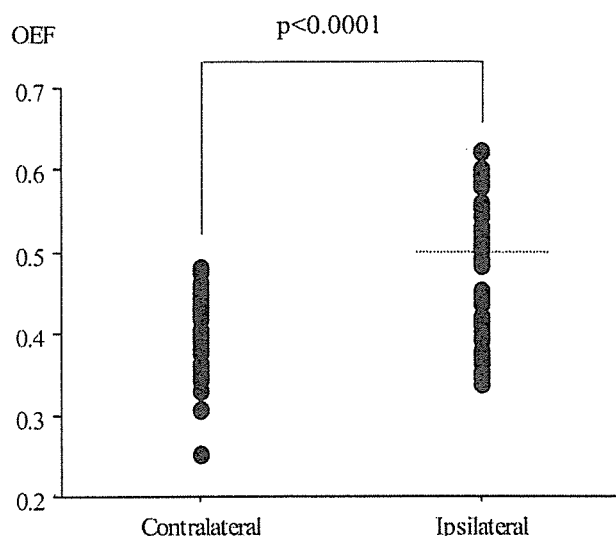


Figure 2. Plot of OEF values in the ipsilateral and contralateral hemisphere of type 3 patients. Dotted line indicates the upper limit of normal OEF value.

can be largely classified into 2 subgroups according to OEF value. OEF was significantly elevated in $\approx 40\%$ of type 3 patients and was within normal limits in the others, indicating that type 3 is not always identical to misery perfusion or stage II. CMRO₂ was significantly higher in patients with elevated OEF than in those with normal OEF (Figure 3A) and significantly correlated with OEF (Figure 1D). Therefore, OEF may depend on the metabolic demand in the ischemic tissue.

As the next step, ¹¹C-FMZ BP and the localization of cerebral infarction were evaluated to specify the underlying pathophysiology of CMRO₂ reduction in the area with type 3 but normal OEF. Subcortical infarction in the ipsilateral hemisphere was not directly related to type 3 but normal OEF, although previous reports suggested its involvement.¹⁵ However, there was a significant correlation between OEF and the ¹¹C-FMZ BP in type 3 patients. Because γ -amino-butyric acid receptors are abundant in the cortex and sensitive to ischemic damage, the specific ligand to their subunits, the central type of benzodiazepine receptors, has been used as a marker of preserved morphological integrity. Garcia et al emphasized the importance of selective neuronal necrosis

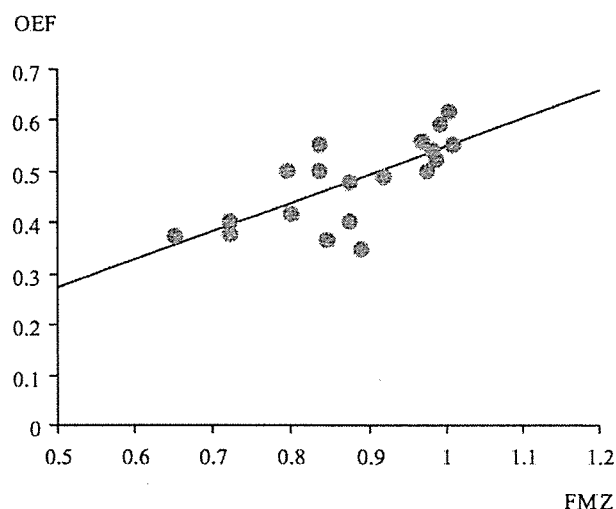


Figure 4. Regression analysis of the relationship between OEF and the BP for ¹¹C-FMZ in 19 type 3 patients.

(incomplete infarction) in human stroke as a pathologic entity.¹⁷ Recently, the authors demonstrated that CMRO₂ and ¹¹C-FMZ BP were reduced to $\approx 80\%$ of the contralateral side, but there was no significant side-to-side difference in CBV and OEF in patients with reduced CBF and normal CVR (type 4) and concluded that type 4 represents oxygen hypometabolism attributable to ischemia-related selective neuronal damage.¹⁶ Previous studies have shown that the patients with type 4 may not be at high risk for subsequent stroke when medically treated.^{6,18} The PET parameters in patients with type 3 ischemia but normal OEF are quite similar to those in the patients with type 4.

Based on these observations, type 3 may include 2 pathophysiologically different conditions: misery perfusion (or stage II ischemia) attributable to hemodynamic compromise, and matched hypometabolism attributable to incomplete infarction. Although the authors have simply graded cerebral hemodynamics of the patients with occlusive carotid artery diseases into 4 types, type 3 should be subdivided into "true type 3," with elevated OEF, and "type 3.5," with normal OEF, in discussing their pathophysiology and long-term prognosis. It is obscure why CVR is impaired in patients with type 3 but normal OEF. As Yamauchi et al pointed out, such

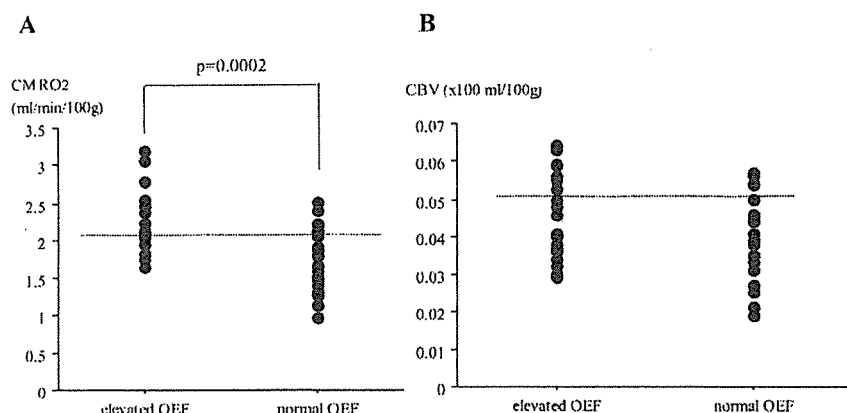


Figure 3. Plots of ipsilateral values of CMRO₂ (A) and CBV (B) in patients with elevated and normal OEF. Dotted lines indicate the lower limit of normal CMRO₂ value (A) and the upper limit of normal CBV value (B).

patients may have complex hemodynamic and metabolic changes in response to both reduced perfusion pressure and ischemic tissue damage.¹⁴

Present results mirror previous descriptions, that is, using $^{133}\text{xenon}$ inhalation method and SPECT, the authors divided 32 patients with ICA occlusion into 4 types and serially measured CBF and CVR after superficial temporal artery to MCA anastomosis. Seven patients were diagnosed as having type 3 before surgery. The CVR normalized in all type 3 patients, suggesting postoperative improvement of cerebral perfusion reserve. But CBF returned to normal range in 3 (42.8%) of 7 type 3 patients. As the result, SPECT parameters altered from type 3 to type 4 in other 4 patients.¹⁸ Furthermore, they recently assessed long-term prognosis of 77 patients who were medically treated because of ICA or MCA occlusion. Of 11 type 3 patients, 4 (36.4%) developed ipsilateral ischemic stroke during follow-up periods.⁶ The present results may explain these varieties in type 3 patients.

However, as recent studies have clarified, hemodynamic and metabolic responses to reduced perfusion pressure are not so simple. Patients with "classic" misery perfusion (elevated OEF and CBV) are at highest risk for subsequent stroke.²² However, CBV changes widely vary in patients with occlusive carotid artery disease. This study also showed that CBV widely varied in spite of OEF values. Further studies would clarify the CBV responses to chronic cerebral ischemia more precisely.

This study showed that type 3 is not equal to misery perfusion. However, SPECT and acetazolamide test are still useful modalities because they can simply select the patients at higher risk for subsequent ischemic stroke at lower costs than PET, as described previously.^{6,7} Thus, it is very valuable to establish the methodology to detect misery perfusion more efficiently with the use of SPECT because PET is not widely available. Based on a significant linear correlation between OEF and ^{11}C -FMZ BP in this study, the authors propose to evaluate whether ^{123}I -iomazenil (IMZ) SPECT can detect misery perfusion or stage II ischemia in type 3 patients more efficiently. ^{123}I -IMZ is an alternative benzodiazepine receptor ligand for SPECT and has been reported that a reduction of its binding reflects oxidative hypometabolism caused by neuronal damage in hemodynamically impaired areas in patients with cerebrovascular disease.²³⁻²⁵ Therefore, SPECT may be able to identify the patients with misery perfusion by measuring CVR and ^{123}I -IMZ binding, if the results on ^{123}I -IMZ SPECT are comparable to those on ^{11}C -FMZ PET in patients with occlusive carotid artery diseases.

Conclusion

Previous studies have shown that type 3 (reduced CBF and CVR) as well as elevated OEF is statistically independent predictors for subsequent stroke in patients with occlusive carotid artery diseases.^{3,4,6,26} However, this study clearly showed that OEF was elevated in $\approx 40\%$ of patients with reduced CBF and CVR (type 3). Significant, positive linear relationships were observed between OEF and CMRO_2 and between OEF and ^{11}C -FMZ BP. Type 3 may include 2 pathophysiologically different conditions: misery perfusion (or stage II) attributable to hemodynamic compromise and

matched hypometabolism attributable to incomplete infarction. Further studies would be necessary to define the SPECT parameter to select the patients at higher risk for subsequent stroke more specifically.

References

1. Baron JC, Boussier MG, Rey A, Guillard A, Comar D, Castaigne P. Reversal of focal "misery-perfusion syndrome" by extra-intracranial arterial bypass in hemodynamic cerebral ischemia. A case study with $^{150}\text{positron}$ emission tomography. *Stroke*. 1981;12:454-459.
2. Powers WJ, Grubb RL Jr, Raichle ME. Physiological responses to focal cerebral ischemia in humans. *Ann Neurol*. 1984;16:546-552.
3. Grubb RL Jr, Derdeyn CP, Fritsch SM, Carpenter DA, Yundt KD, Videen TO, Spitznagel EL, Powers WJ. Importance of hemodynamic factors in the prognosis of symptomatic carotid occlusion. *J Am Med Assoc*. 1998;280:1055-1060.
4. Yamauchi H, Fukuyama H, Nagahama Y, Nabatame H, Ueno M, Nishizawa S, Konishi J, Shio H. Significance of increased oxygen extraction fraction in five-year prognosis of major cerebral arterial occlusive diseases. *J Nucl Med*. 1999;40:1992-1998.
5. Derdeyn CP, Videen TO, Grubb RL Jr, Powers WJ. Comparison of pet oxygen extraction fraction methods for the prediction of stroke risk. *J Nucl Med*. 2001;42:1195-1197.
6. Kuroda S, Houkin K, Kamiyama H, Mitsumori K, Iwasaki Y, Abe H. Long-term prognosis of medically treated patients with internal carotid or middle cerebral artery occlusion: can acetazolamide test predict it? *Stroke*. 2001;32:2110-2116.
7. Ogasawara K, Ogawa A, Yoshimoto T. Cerebrovascular reactivity to acetazolamide and outcome in patients with symptomatic internal carotid or middle cerebral artery occlusion: a xenon-133 single-photon emission computed tomography study. *Stroke*. 2002;33:1857-1862.
8. Nemoto EM, Yonas H. Revisiting the question, "is the acetazolamide test valid for quantitative assessment of maximal cerebral autoregulatory vasodilation?" *Stroke*. 2001;32:1234-1237.
9. Kanno I, Uemura K, Higano S, Murakami M, Iida H, Miura S, Shishido F, Inugami A, Sayama I. Oxygen extraction fraction at maximally vasodilated tissue in the ischemic brain estimated from the regional CO_2 responsiveness measured by positron emission tomography. *J Cereb Blood Flow Metab*. 1988;8:227-235.
10. Herold S, Brown MM, Frackowiak RS, Mansfield AO, Thomas DJ, Marshall J. Assessment of cerebral haemodynamic reserve: correlation between pet parameters and CO_2 reactivity measured by the intravenous $^{133}\text{xenon}$ injection technique. *J Neurol Neurosurg Psychiatry*. 1988;51:1045-1050.
11. Hirano T, Minematsu K, Hasegawa Y, Tanaka Y, Hayashida K, Yamaguchi T. Acetazolamide reactivity on ^{123}I -IMP single photon emission computed tomography in patients with major cerebral artery occlusive disease: correlation with positron emission tomography parameters. *J Cereb Blood Flow Metab*. 1994;14:763-770.
12. Imaizumi M, Kitagawa K, Hashikawa K, Oku N, Teratani T, Takasawa M, Yoshikawa T, Rishu P, Ohtsuki T, Hori M, Matsumoto M, Nishimura T. Detection of misery perfusion with split-dose ^{123}I -iodoamphetamine single-photon emission computed tomography in patients with carotid occlusive diseases. *Stroke*. 2002;33:2217-2223.
13. Nariai T, Suzuki R, Hirakawa K, Maehara T, Ishii K, Senda M. Vascular reserve in chronic cerebral ischemia measured by the acetazolamide challenge test: comparison with positron emission tomography. *AJNR Am J Neuroradiol*. 1995;16:563-570.
14. Yamauchi H, Okazawa H, Kishibe Y, Sugimoto K, Takahashi M. Oxygen extraction fraction and acetazolamide reactivity in symptomatic carotid artery disease. *J Neurol Neurosurg Psychiatry*. 2004;75:33-37.
15. Nemoto EM, Yonas H, Kuwabara H, Pindzola RR, Sashin D, Meltzer CC, Price JC, Chang Y, Johnson DW. Identification of hemodynamic compromise by cerebrovascular reserve and oxygen extraction fraction in occlusive vascular disease. *J Cereb Blood Flow Metab*. 2004;24:1081-1089.
16. Kuroda S, Shiga T, Ishikawa T, Houkin K, Narita T, Katoh C, Tamaki N, Iwasaki Y. Reduced blood flow and preserved vasoreactivity characterize oxygen hypometabolism due to incomplete infarction in occlusive carotid artery diseases. *J Nucl Med*. 2004;45:943-949.
17. Garcia JH, Lassen NA, Weiller C, Sperling B, Nakagawara J. Ischemic stroke and incomplete infarction. *Stroke*. 1996;27:761-765.